Supporting Information

$[MW_{12}O_{44}]$ cluster: unprecedented central heteroatoms atomically dispersed in eight coordination state bridging 1:12 polyoxometalate family of Keggin and Silverton

Yongdong Chen[a,b], Shanli Tian[a,b], Zhaoxian Qin[b], Jiangwei Zhang[b,*] Youhai Cao[b], Shengqi Chu[c], Lanlu Lu[d], and Gao Li[b,*]

[a.]College of Chemistry and Chemical Engineering, Southwest Petroleum University, Chengdu 610500, Sichuan, China.

[b.]State Key Laboratory of Catalysis, Dalian Institute of Chemical Physics, Chinese Academy of Sciences, Dalian 116023, China. E-mail: jwzhang@dicp.ac.cn (J.Z.); gaoli@dicp.ac.cn (G.L.).

[c.]Beijing Synchrotron Radiation Facility, Institute of High Energy Physics, Chinese Academy of Sciences, Beijing 100049, China.

[d.]Shanghai Advanced Research Institute, Chinese Academy of Sciences, Shanghai 201210, China

Experimental

Synthesis of $(NH_4)_{10}H_4[NiW_{12}O_{44}]$

$(NH_4)_{10}H_2W_{12}O_{42}$ (3.060 g, 1 mmol) was dissolved in 35 mL H_2O then the solution was acidized by HNO_3 to pH 2.5 and refluxing for 1h. The 15ml 1M Glycine-hydrochloric acid buffer was added to provide precise and stable pH control at 2.5, and $Ni(NO_3)_2$ (0.18g 1mmol) was added, the solution was kept at 80 °C for 0.5h. Then the solution was evaporated to dryness. The title compound could be obtained as pale blue crystalline products with the yield about 80% based on W. Suitable single crystals for X-ray diffraction were grown by slow evaporation. Crystal

data and structure refinement: $(NH_4)_{10}H_4[NiW_{12}O_{44}]$: I*m-3m*, a=17.6345 Å, V=5483.9 Å^3, Z=2, 517 reflections measured, R_1=0.0649, wR_2=0.1645.

Synthesis of $(NC_{16}H_{36})_4(NH_4)_{10}[NiW_{12}O_{44}]$

$(NC_{16}H_{36})_4(NH_4)_{10}[NiW_{12}O_{44}]$ was obtained by cation exchange: $(NH_4)_{10}H_4[NiW_{12}O_{44}]$ (0.788g, 0.25 mmol) was dissolved in 15 mL H_2O then 5ml $(NC_{16}H_{36})Br$ aqueous was added (0.322, 1mmol), through vigorous stir The title compound was formed and separated by filtration as pale blue precipitate.

$C_{64}H_{184}N_{14}O_{44}NiW_{12}$, M_r =4118.98. C: N: Ni: W=63.86:13.73:1:12.04. IR (cm^{-1}): 3849, 3746, 3446, 2954, 2874, 1636, 1471, 1382, 1157, 1068, 960, 890, 806. UV-Vis (H_2O, nm): λ_{LMCT}=263, $\lambda_{d\text{-}d}$=630.

Synthesis of $(NH_4)_{10}H_4[CoW_{12}O_{44}]$ and $(NC_{16}H_{36})_4(NH_4)_{10}[CoW_{12}O_{44}]$

The synthesis process is similar to the synthesis of compound **1** while used $Co(NO_3)_2$ instead of $Ni(NO_3)_2$. $(NH_4)_{10}H_4[CoW_{12}O_{44}]$ could be obtained as pale pink crystalline products with the yield about 78% based on W. Crystal data and structure refinement: $(NH_4)_{10}H_4[CoW_{12}O_{44}]$: I*m-3m*, a=17.555 Å, V=5410.1 Å^3, Z=2, 515 reflections measured, R_1=0.0585, wR_2=0.1946.

$C_{64}H_{184}N_{14}O_{44}CoW_{12}$, M_r =4119.22. C: N: Co: W=64.36:14.21:1:11.94. IR (cm^{-1}): 3849, 3741, 3432, 2963, 2874, 1641, 1471, 1373, 1152, 1064, 951, 890, 815. UV-Vis (H_2O, nm): λ_{LMCT}=263, $\lambda_{d\text{-}d}$=523.

Synthesis of $(NH_4)_9H_4[FeW_{12}O_{44}]$ and $(NC_{16}H_{36})_4(NH_4)_9[FeW_{12}O_{44}]$

The synthesis process is similar to the synthesis of compound **1** while used $Fe(NO_3)_3$ instead of $Ni(NO_3)_2$. $(NH_4)_9H_4[FeW_{12}O_{44}]$ could be obtained as white crystalline products with the yield about 81% based on W. Crystal data and structure refinement: $(NH_4)_9H_4[FeW_{12}O_{44}]$: I*m-3m*, a=17.5944 Å, V=5446.6 Å^3, Z=2, 516 reflections measured, R_1=0.1002, wR_2=0.2166.

$C_{64}H_{180}N_{13}O_{44}FeW_{12}$, M_r =4098.10. C: N: Fe: W=63.86:13.32:1:11.96. IR (cm^{-1}): 3854, 3741, 3437, 2958, 2874, 1641, 1476, 1378, 1158, 1064, 956, 890, 810. UV-Vis (H_2O, nm): λ_{LMCT}=263.

Synthesis of $(NH_4)_{10}H_6[W_{12}O_{44}]$

$(NH_4)_{10}H_2W_{12}O_{42}$ (3.060 g, 1 mmol) was dissolved in 35 mL H_2O then the solution was acidized by HNO_3 to pH 2.5 and refluxing for 1h. Then the solution was evaporated to dryness. The title compound could be obtained as white crystalline products. Suitable single crystals for X-ray diffraction were grown by slow evaporation. Crystal data and structure refinement: $(NH_4)_{10}H_6[W_{12}O_{44}]$: I-*43m*, a=17.6345 Å, V=5483.9 $Å^3$, Z=2, 857 reflections measured, R_1=0.0889, wR_2=0.2290.

XAFS analysis

The EXAFS spectra were obtained by subtracting the post-edge background from the overall absorption and then normalizing with respect to the edge-jump step. Subsequently, the χ(k) data of were Fourier transformed to real (R) space using a hanning windows (dk=1.0 Å-1) to separate the EXAFS contributions from different coordination shells. To obtain the quantitative structural parameters around central atoms, least-squares curve parameter fitting was performed using the ARTEMIS module of Demeter software packages

The following EXAFS equation was used:

$$\chi(k)=\sum_j \frac{N_j S_o^2 F_j(k)}{k R_j^2}\exp[-2k^2\sigma_j^2]\exp[\frac{-2R_j}{\lambda(k)}]\sin[2kR_j+\phi_j(k)]$$

S_0^2 is the amplitude reduction factor, $F_j(k)$ is the effective curved-wave backscattering amplitude, N_j is the number of neighbors in the j^{th} atomic shell, R_j is the distance between the Xray absorbing central atom and the atoms in the j^{th} atomic shell (backscatterer), λ is the mean free path in Å, $\phi_j(k)$ is the phase shift (including the phase shift for each shell and the total central atom phase shift), σ_j is the Debye-Waller parameter of the j^{th} atomic shell (variation of distances around the average R_j). The functions $F_j(k)$, λ and $\phi_j(k)$ were calculated with the ab initio code FEFF. The additional details for EXAFS simulations are given below.

The coordination numbers of model samples were fixed as the nominal values. The obtained S_0^2 was fixed in the subsequent fitting. While the internal atomic distances R, Debye-Waller factor σ^2, and the edge-energy shift ΔE_0 were allowed to run freely.

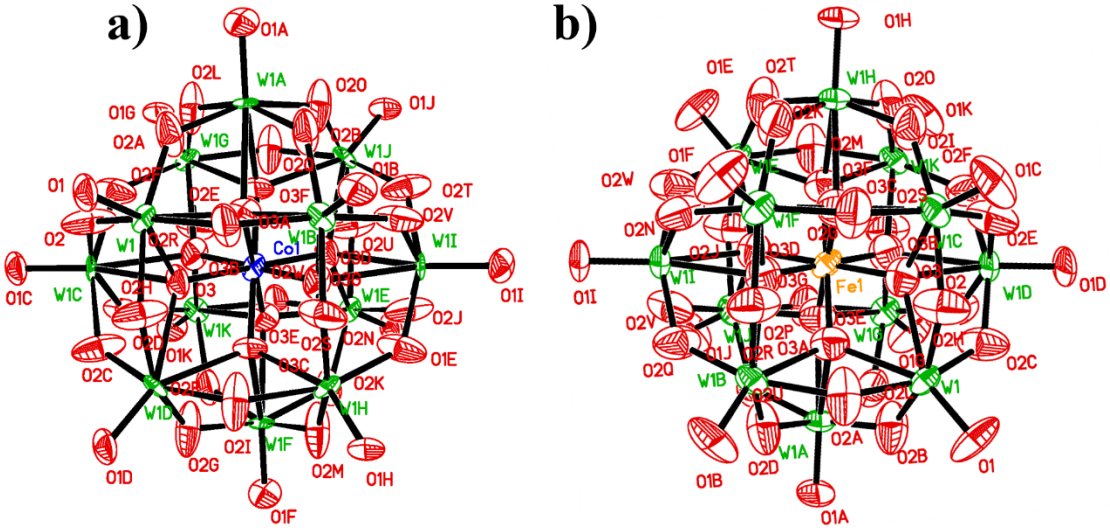

Figure S1a. ORTEP drawings of cluster anions of $[CoW_{12}O_{44}]$ (a) and $[FeW_{12}O_{44}]$ (b). Thermal ellipsoids are drawn at the 30% probability level through symmetric operation of minimum asymmetric unit of MWO_3.

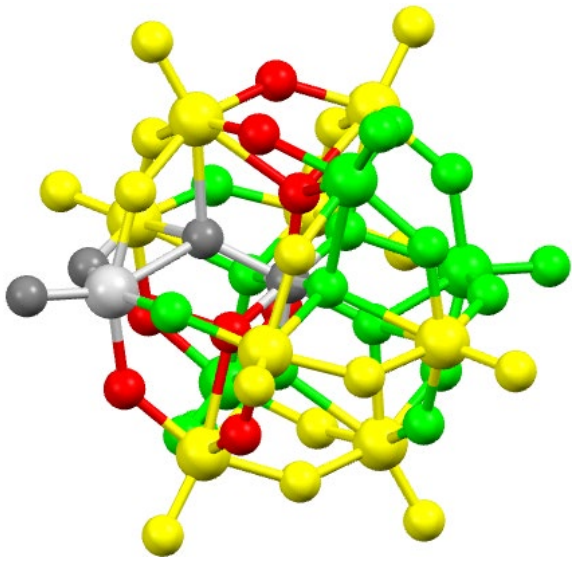

Figure S1b. The formation of $[NiW_{12}O_{44}]$ nanocluster from the minimum asymmetric unit of $NiWO_3$ (the grey fragment) through color symmetric operation

The color symmetric operation code is list as following:

'x, y, z'

'-x, -y, z'

'-x, y, -z'

'x, -y, -z'

'z, x, y'

'z, -x, -y'

'-z, -x, y'

'-z, x, -y'

'y, z, x'

'-y, z, -x'

'y, -z, -x'

'-y, -z, x'

'y, x, z'

'-y, -x, z'

'y, -x, -z'

'-y, x, -z'

'x, z, y'

'-x, z, -y'

'-x, -z, y'

'x, -z, -y'

'z, y, x'

'z, -y, -x'

'-z, y, -x'

'-z, -y, x'

'x+1/2, y+1/2, z+1/2'

'-x+1/2, -y+1/2, z+1/2'

'-x+1/2, y+1/2, -z+1/2'

'x+1/2, -y+1/2, -z+1/2'

'z+1/2, x+1/2, y+1/2'

'z+1/2, -x+1/2, -y+1/2'

'-z+1/2, -x+1/2, y+1/2'

'-z+1/2, x+1/2, -y+1/2'

'y+1/2, z+1/2, x+1/2'

'-y+1/2, z+1/2, -x+1/2'

'y+1/2, -z+1/2, -x+1/2'

'-y+1/2, -z+1/2, x+1/2'

'y+1/2, x+1/2, z+1/2'

'-y+1/2, -x+1/2, z+1/2'

'y+1/2, -x+1/2, -z+1/2'

'-y+1/2, x+1/2, -z+1/2'

'x+1/2, z+1/2, y+1/2'

'-x+1/2, z+1/2, -y+1/2'

'-x+1/2, -z+1/2, y+1/2'

'x+1/2, -z+1/2, -y+1/2'

'z+1/2, y+1/2, x+1/2'

'z+1/2, -y+1/2, -x+1/2'

'-z+1/2, y+1/2, -x+1/2'

'-z+1/2, -y+1/2, x+1/2'

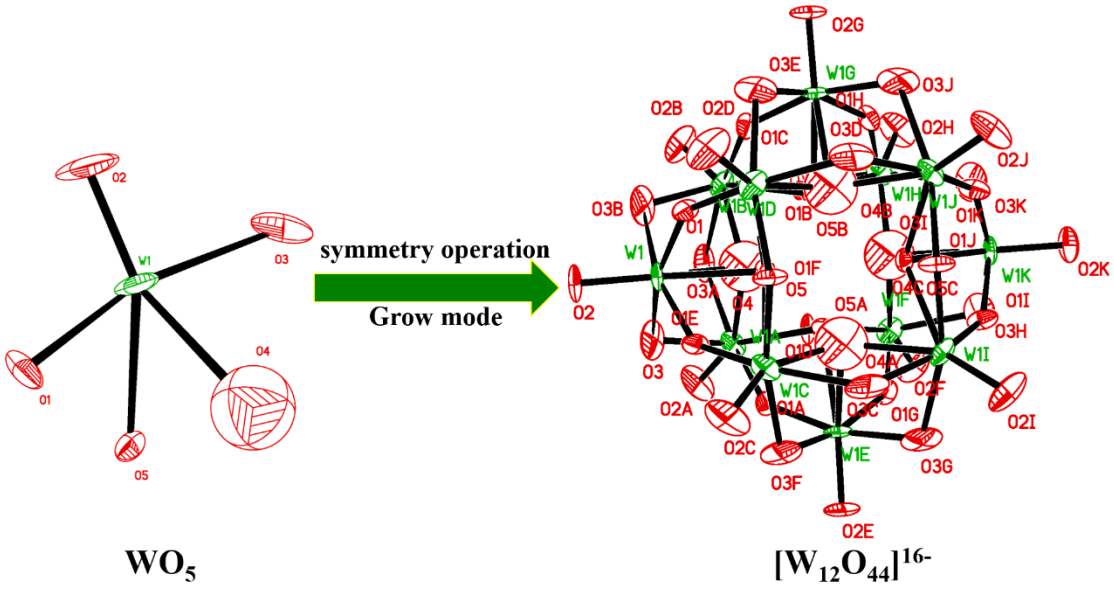

Figure S2a. ORTEP drawings of cluster anions of $[W_{12}O_{44}]^{16-}$. Thermal ellipsoids are drawn at the 30% probability level through symmetric operation of minimum asymmetric unit of WO_5.

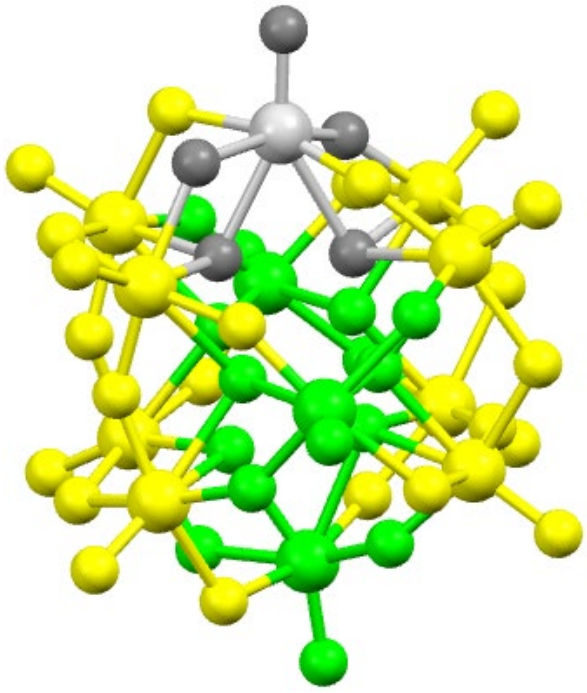

Figure S2b. The formation of $[W_{12}O_{44}]^{16-}$ nanocluster from the minimum asymmetric unit of WO_5 (the grey fragment) through Color symmetric operation.

The color symmetric operation code is list as following:

'x, y, z'

'-x, -y, z'

'-x, y, -z'

'x, -y, -z'

'z, x, y'

'z, -x, -y'

'-z, -x, y'

'-z, x, -y'

'y, z, x'

'-y, z, -x'

'y, -z, -x'

'-y, -z, x'

'y, x, z'

'-y, -x, z'

'y, -x, -z'

'-y, x, -z'

'x, z, y'

'-x, z, -y'

'-x, -z, y'

'x, -z, -y'

'z, y, x'

'z, -y, -x'

'-z, y, -x'

'-z, -y, x'

'x+1/2, y+1/2, z+1/2'

'-x+1/2, -y+1/2, z+1/2'

'-x+1/2, y+1/2, -z+1/2'

'x+1/2, -y+1/2, -z+1/2'

'z+1/2, x+1/2, y+1/2'

'z+1/2, -x+1/2, -y+1/2'

'-z+1/2, -x+1/2, y+1/2'

'-z+1/2, x+1/2, -y+1/2'

'y+1/2, z+1/2, x+1/2'

'-y+1/2, z+1/2, -x+1/2'

'y+1/2, -z+1/2, -x+1/2'

'-y+1/2, -z+1/2, x+1/2'

'y+1/2, x+1/2, z+1/2'

'-y+1/2, -x+1/2, z+1/2'

'y+1/2, -x+1/2, -z+1/2'

'-y+1/2, x+1/2, -z+1/2'

'x+1/2, z+1/2, y+1/2'

'-x+1/2, z+1/2, -y+1/2'

'-x+1/2, -z+1/2, y+1/2'

'x+1/2, -z+1/2, -y+1/2'

'z+1/2, y+1/2, x+1/2'

'z+1/2, -y+1/2, -x+1/2'

'-z+1/2, y+1/2, -x+1/2'

'-z+1/2, -y+1/2, x+1/2'

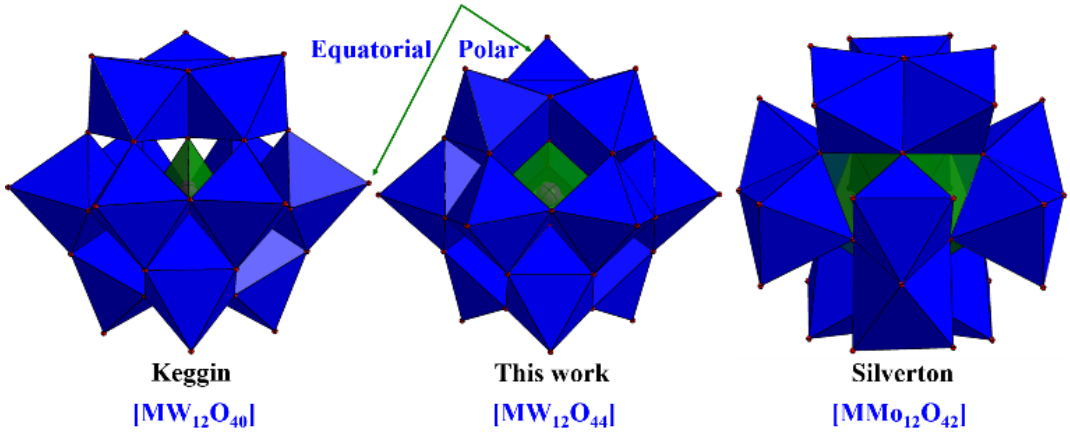

Figure S3. polyhedron of 1:12 hetero-polyoxometalates with different central heteroatom configuration: tetrahedron for Keggin, hexahedron for [$MW_{12}O_{44}$]; icosahedron for Silverton.

6 WO_6 octahedrons surrounded around the central heteroatom polyhedron in approximate plane defined as equatorial position; (ii) each 3 WO_6 octahedrons in the up and down plane defined as polar position.

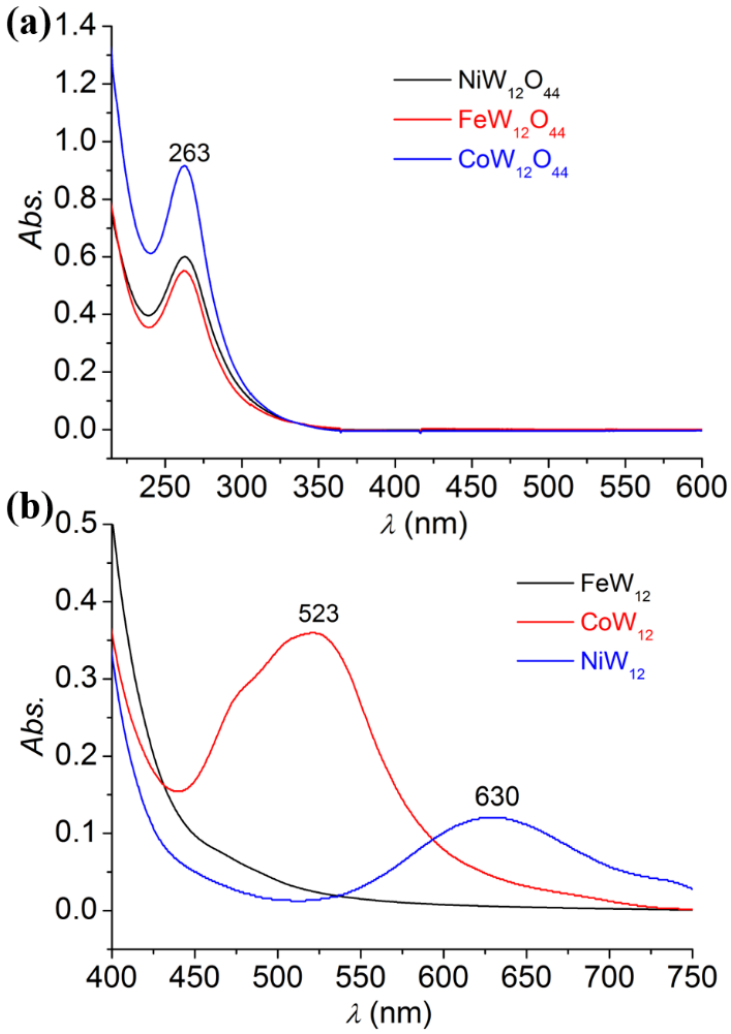

Figure S4. UV/Vis spectra of [$MW_{12}O_{44}$] clusters: (a) LMCT absorption and (b) d-d transition absorption spectra.

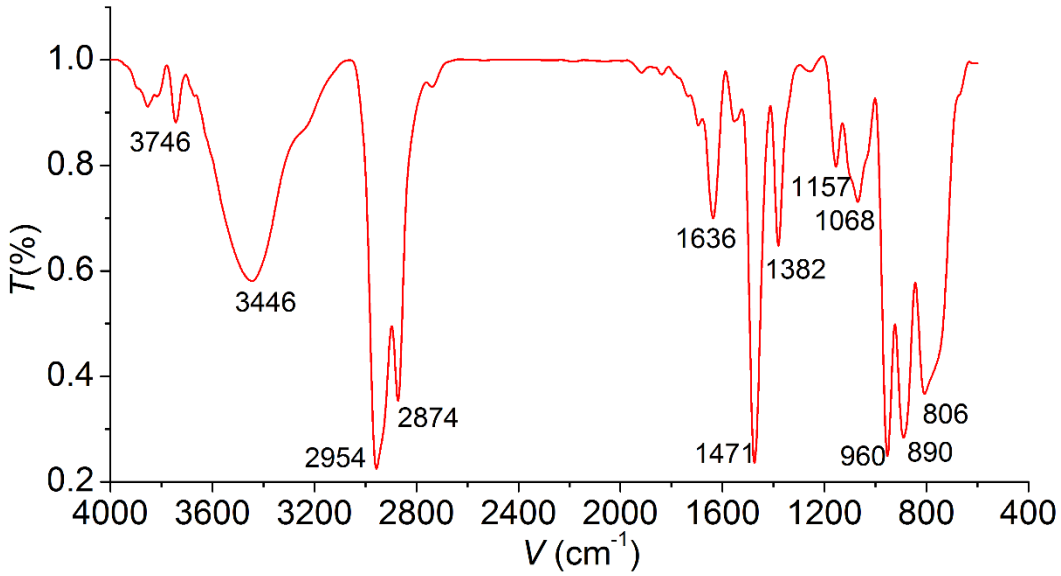

Figure S5a. The FT-IR spectrum of $(NC_{16}H_{36})_4(NH_4)_{10}[NiW_{12}O_{44}]$.

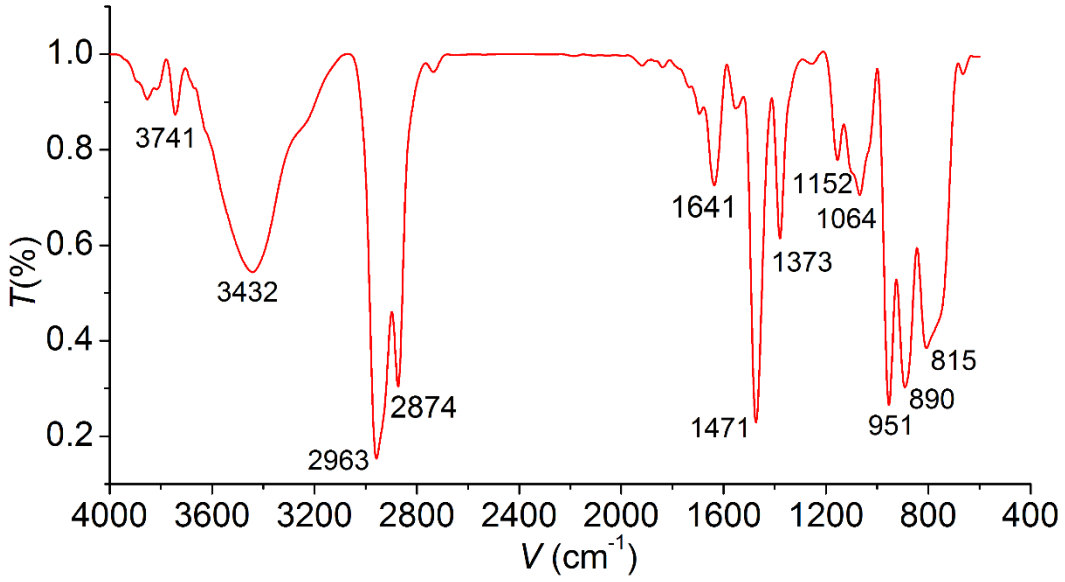

Figure S5b. The FT-IR spectrum of $(NC_{16}H_{36})_4(NH_4)_{10}[CoW_{12}O_{44}]$.

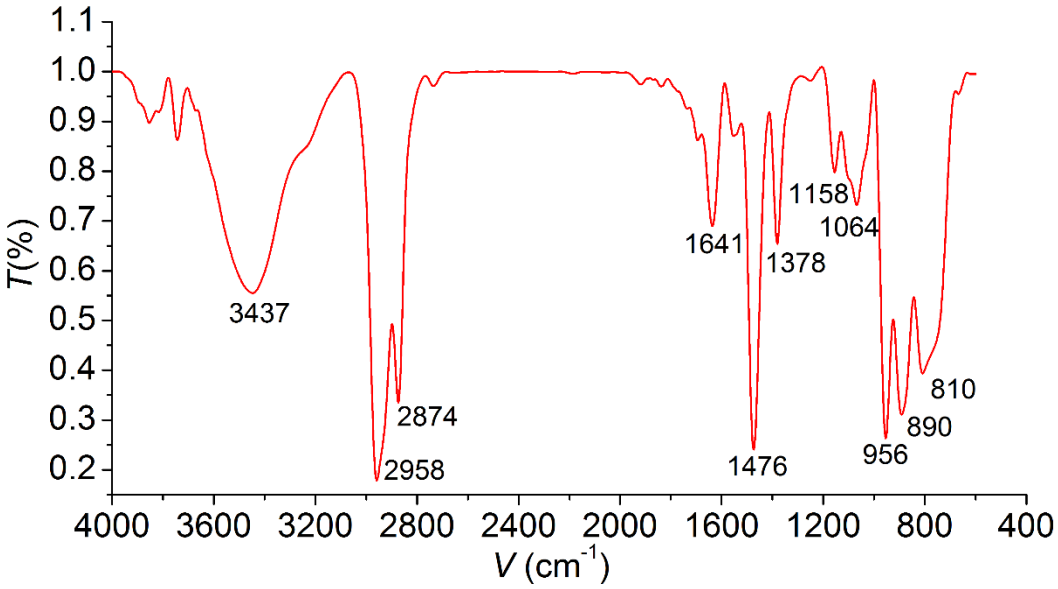

Figure S5c. The FT-IR spectrum of $(NC_{16}H_{36})_4(NH_4)_9[FeW_{12}O_{44}]$.

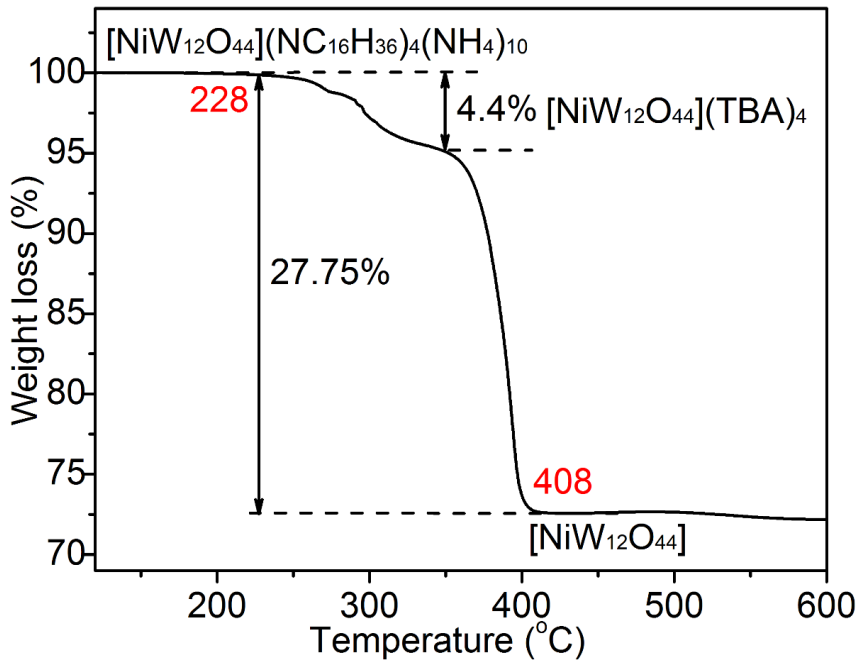

Figure S6a. TGA analysis of $(NC_{16}H_{36})_4(NH_4)_{10}[NiW_{12}O_{44}]$.

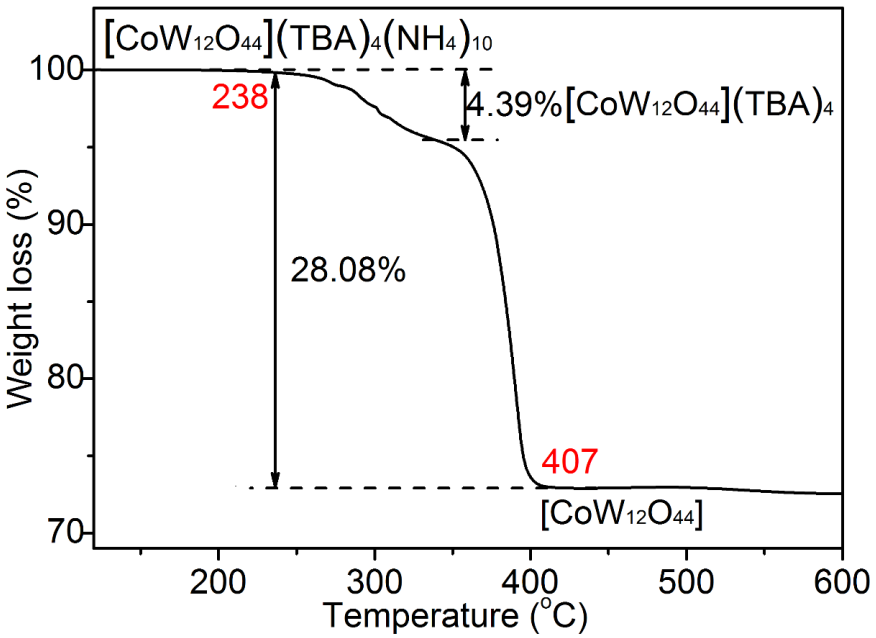

Figure S6b. TGA analysis of $(NC_{16}H_{36})_4(NH_4)_{10}[CoW_{12}O_{44}]$.

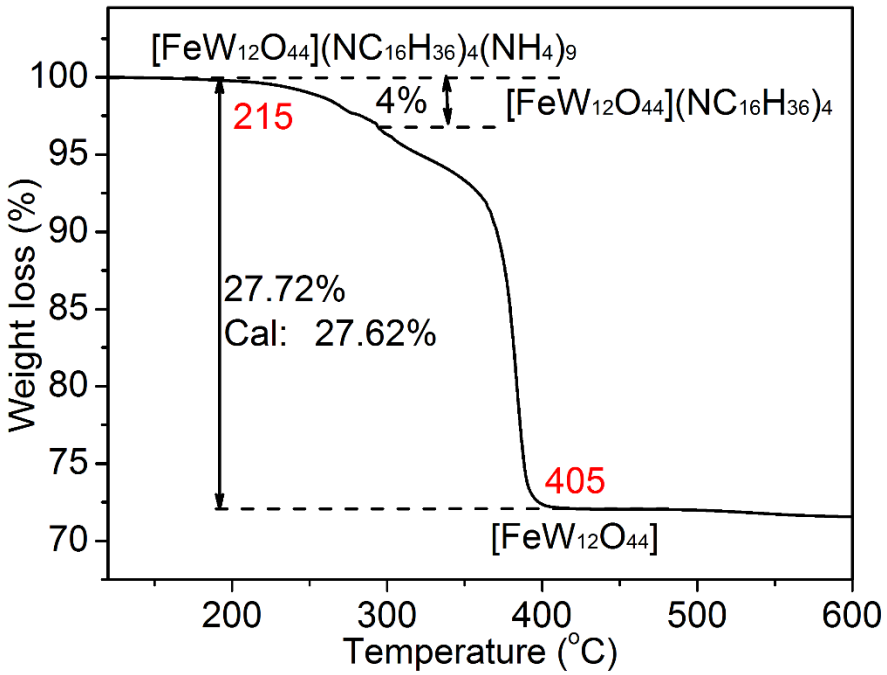

Figure S6c. TGA analysis of $(NC_{16}H_{36})_4(NH_4)_9[FeW_{12}O_{44}]$

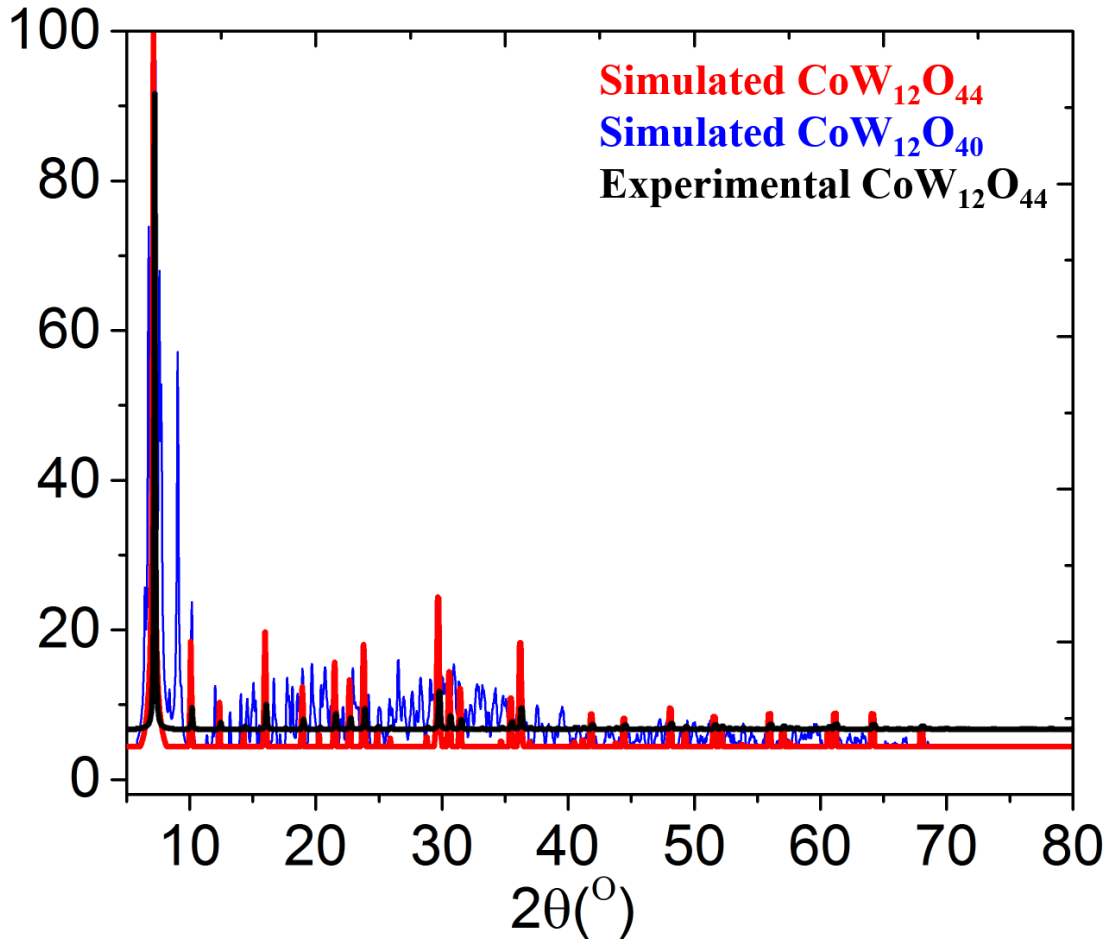

Figure S7a. The simulated and experimental powder XRD pattern of [$CoW_{12}O_{44}$] and the simulated powder XRD pattern of [$CoW_{12}O_{40}$] respectively

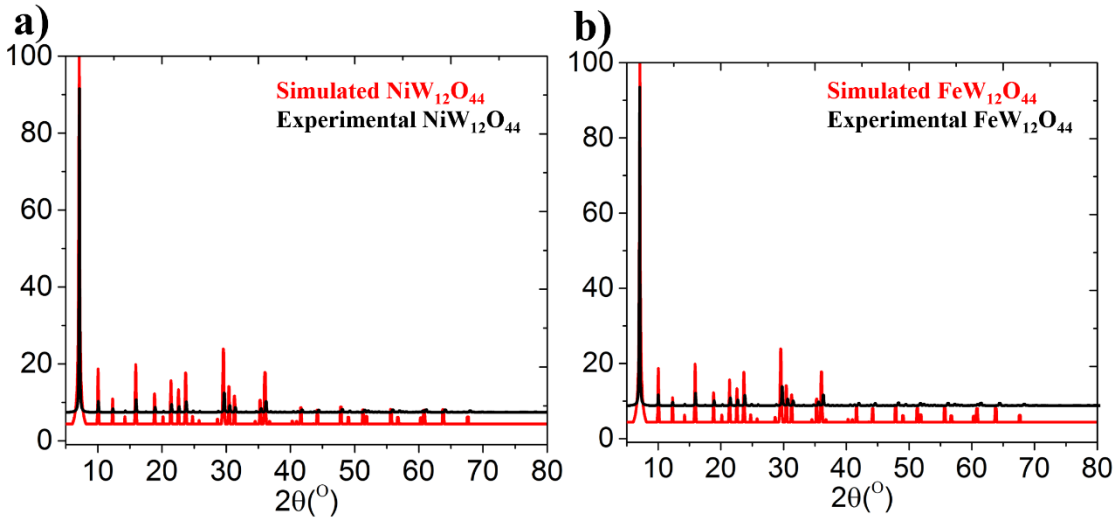

Figure S7b. The simulated and experimental powder XRD pattern of [$NiW_{12}O_{44}$] (a) and [$FeW_{12}O_{44}$] (b) respectively